Kallikrein 6 Induces E-Cadherin Shedding and Promotes Cell Proliferation, Migration, and Invasion

Britta Klucky,[1] Regina Mueller,[1] Ingeborg Vogt,[1] Sibylle Teurich,[1] Bettina Hartenstein,[1] Kai Breuhahn,[2] Christa Flechtenmacher,[2] Peter Angel,[1] and Jochen Hess[1]

[1]Division of Signal Transduction and Growth Control, Deutsches Krebsforschungszentrum; [2]Institut of Pathology, University Hospital, Heidelberg, Germany

Abstract

Recently, we described phorbol ester–induced expression of the brain and skin serine proteinase Bssp/kallikrein 6 (Klk6), the mouse orthologue of human KLK6, in mouse back skin and in advanced tumor stages of a well-established multistage tumor model. Here, we show KLK6 up-regulation in squamous skin tumors of human patients and in tumors of other epithelial tissues. Ectopic Klk6 expression in mouse keratinocyte cell lines induces a spindle-like morphology associated with accelerated proliferation, migration, and invasion capacity. We found reduced E-cadherin protein levels in the cell membrane and nuclear translocation of β-catenin in Klk6-expressing mouse keratinocytes and human HEK293 cells transfected with a KLK6 expression plasmid. Additionally, HEK293 cells exhibited induced T-cell factor–dependent transcription and impaired cell-cell adhesion in the presence of KLK6, which was accompanied by induced E-cadherin ectodomain shedding. Interestingly, tissue inhibitor of metalloproteinase (TIMP)-1 and TIMP-3 interfere with KLK6-induced E-cadherin ectodomain shedding and rescue the cell-cell adhesion defect *in vitro*, suggesting the involvement of matrix metalloproteinase and/or a disintegrin and metalloproteinase (ADAM) proteolytic activity. In line with this assumption, we found increased levels of the mature 62-kDa ADAM10 proteinase in cells expressing ectopic KLK6 compared with mock controls. Finally, enhanced epidermal keratinocyte proliferation and migration in concert with decreased E-cadherin protein levels are confirmed in an *in vivo* Klk6 transgenic mouse model. [Cancer Res 2007; 67(17):8198–206]

Introduction

Cancer is a multistage disorder in which genetic and epigenetic changes result in characteristic alterations within the gene regulatory network, thereby influencing the cellular decision of differentiation, proliferation, or survival (1). Gene deregulation enables a cancer cell to achieve essential alterations on its way to malignancy, such as growth signal self-sufficiency, insensitivity to growth-inhibitory signals, evasion of programmed cell death, unlimited replication potential, sustained angiogenesis, and tissue invasion and metastasis (2). One of the best-established *in vivo* models for multistage carcinogenesis is the chemically induced tumor model of mouse back skin, in which tumor initiation is achieved by the mutagen 7,12-dimethylbenz(a)anthracene and tumor promotion is driven by phorbol esters, such as 12-*O*-tetradecanoylphorbol-13-acetate (TPA; refs. 3, 4). Recently, we applied global gene expression analysis on samples derived from distinct tumor stages and could identify a comprehensive list of novel tumor-associated genes (5–10). One of the differentially expressed genes showing enhanced expression in advanced tumor stages encodes the brain and skin serine proteinase Bssp [also known as kallikrein 6 (Klk6) according to the recommendation for future nomenclature of kallikrein-related peptidases (11)]. Klk6 is the mouse orthologue of human KLK6 that belongs to a large family of kallikrein-related peptidases, representing secreted serine proteinases with diverse expression patterns and functions in cell physiology (12, 13). There is substantial evidence for aberrant expression of kallikreins in common human tumor types, and therefore, most studies in the past focused on their clinical application as biomarkers (12). However, emerging experimental data suggest a causal role of kallikrein family members in tumorigenesis, and one can assume that understanding their *in vivo* function will represent a novel research avenue expanding our knowledge of neoplastic progression. This should allow the development of innovative strategies for cancer therapy. In the current study, we show KLK6 up-regulation in human cutaneous skin cancer associated with malignant progression and in tumors of other epithelial tissues. Ectopic Klk6 expression in a mouse keratinocyte cell line promotes cell proliferation, migration, and invasion, most likely due to impaired E-cadherin–mediated cell-cell adhesion and β-catenin accumulation in the nucleus. Analysis of cutaneous wound healing in a Klk6 transgenic mouse model confirms its crucial role in keratinocyte proliferation and migration as well as in E-cadherin protein processing *in vivo*. Interestingly, the tissue inhibitor of metalloproteinase (TIMP)-1 and TIMP-3 interfere with induced E-cadherin ectodomain shedding and restore cell-cell adhesion in the presence of KLK6, which shows the involvement of proteolytic active matrix metalloproteinases (MMPs).

Materials and Methods

Generation of tissue microarrays. Samples of the National Center for Tumor Diseases Heidelberg were used for preparation of tissue microarrays (Institutional Commission of Ethics AZ 206/207). They were fixed in 10% buffered formalin and embedded in paraffin followed by conventional preparation of 3-μm sections and H&E staining. Vital tumor regions were identified by a pathologist and used for punch cylinder (1 mm) transfer from donor to recipient paraffin blocks using a tissue-arraying instrument (Becher Instruments). Consecutive sections (5 μm) of the recipient blocks were made with a conventional microtome and processed according to the manufacturer's instructions. A total of 103 tissues was obtained for this

Note: Supplementary data for this article are available at Cancer Research Online (http://cancerres.aacrjournals.org/).

Requests for reprints: Peter Angel, Division of Signal Transduction and Growth Control, Deutsches Krebsforschungszentrum, Im Neuenheimer Feld 280, D-69120 Heidelberg, Germany. Phone: 49-6221-42-4570; Fax: 49-6221-42-4554; E-mail: p.angel@dkfz.de.

doi:10.1158/0008-5472.CAN-07-0607

study, including 7 samples of nonaffected skin, 39 samples of premalignant tumors (carcinoma *in situ* and actinic keratosis), and 57 samples of cutaneous squamous cell carcinoma (SCC).

Cancer profiling array. A *KLK6*-specific cDNA probe (299–771 bp from NM_001012964) was labeled with [α-^{32}P]dCTP by random primer labeling (Rediprime kit, Amersham Biosciences) and purified using push columns (Stratagene Europe). Hybridization of the Cancer Profiling Array II (BD Biosciences) was done according to the manufacturer's protocol. The specificity of the *KLK6*-specific cDNA probe was verified by Northern blot analysis of total RNA from different human keratinocyte cell lines (data not shown).

Cell lines and culture conditions. The mouse keratinocyte cell line MCA3D was cultured in α-MEM (Cambrex Bio Science) supplemented with 10% FCS (Sigma) and 2 mmol/L L-glutamine (Cambrex Bio Science) at 34°C in a humidified atmosphere of 6% CO_2. HEK293 cells were maintained in DMEM (Cambrex Bio Science) supplemented with 10% FCS (Sigma) at 37°C in a humidified atmosphere of 6% CO_2. To establish stable MCA3D clones, 7×10^6 cells were transfected with 10 μg parental pcDNA3.1-His/Myc or pcDNA3.1-Klk6-Myc/His plasmids. Transfection was done by electroporation (450 kV and 500 μF) in a 0.4-cm gap cuvette using a GenePulser (Bio-Rad Laboratories). Transfected cells were selected for 14 days with 0.8 mg/mL geneticin (PAA Laboratories), single clones were picked, and genomic transgene integration was confirmed by PCR analysis (data not shown).

Plasmids, transient transfection, and reporter gene assay. The coding sequence of mouse *Klk6* (217–978 bp from NM_011177) and human *KLK6* (273–995 bp from NM_001012964) were amplified by PCR and cloned in pcDNA3.1-Myc/His version A (Invitrogen) linearized with *Hin*dIII and *Xho*I. The stop codon of both genes was mutated to enable expression of Myc/His fusion proteins. HEK293 cells were transiently transfected by the calcium phosphate protocol done as described elsewhere (14). For T-cell factor (TCF) reporter gene assays, HEK293 cells were transfected with pcDNA3.1-KLK6-Myc/His or the parental plasmid together with the TCFwt-luciferase reporter plasmid (TOPflash) and TCFmut-luciferase reporter plasmid (FOPflash; Chemicon). A plasmid carrying the *Renilla luciferase* gene under the control of the human cytomegalovirus immediate-early enhancer promoter region was cotransfected as an internal control (Promega). Twenty-four hours after transfection, cells were harvested and reporter gene assays were done using the Dual-Luciferase Assay System (Promega). Transient transfection and luciferase reporter gene assays were done five times. For inhibition studies, recombinant TIMP-1 and TIMP-3 proteins (Biomol) were added to transiently transfected HEK293 cells at the indicated concentrations.

RNA extraction, cDNA synthesis, and reverse transcription-PCR analysis. Total RNA from cell lines was isolated with RNApure following the manufacturer's instructions (PeqLab Biotechnology). cDNA synthesis and semiquantitative reverse transcription-PCR (RT-PCR) were described previously (8). Sequences of specific primers are available on request.

Protein extraction, purification, and analysis. Preparation of whole-cell extracts was done with radioimmunoprecipitation assay buffer [50 mmol/L Tris-HCl (pH 8.0), 150 mmol/L NaCl, 0.1% SDS, 0.5% sodium deoxycholate, 1% NP40, proteinase inhibitor cocktail], and purification of His-tagged Klk6 protein was done with Talon metal affinity resin according to the manufacturer's instructions (BD Biosciences). Extraction of nuclear and cytoplasmic proteins for Western blot analysis was done as described elsewhere (15). Purification of soluble E-cadherin from cell culture supernatants with concanavalin A (ConA)-Sepharose (Sigma) and Western blot analysis was described previously (14, 16), and the antibodies that were used are listed in Supplementary Table S1. ELISA assays for soluble E-cadherin were carried out according to the manufacturer's instructions (TaKaRa).

Gelatin zymography. Conditioned medium of mock- or KLK6-transfected HEK293 cells were loaded under nonreducing conditions onto a 10% SDS-polyacrylamide gel containing 1 mg/mL gelatin. After electrophoresis and washing the gel with Triton X-100 (2.5% v/v, twice for 30 min), the gel was incubated in MMP reaction buffer [50 mmol/L Tris-HCl (pH 7.8), 200 mmol/L NaCl, 5 mmol/L $CaCl_2$] at 37°C for 16 h. As a control for MMP gelatinolytic activity, 5 mmol/L EDTA was added to the MMP reaction buffer. Gelatinolytic activity was detected as transparent bands on staining with Coomassie Brilliant Blue G-250 solution and incubation in destaining solution (10% acetic acid, 20% methanol).

Immunohistochemistry and immunofluorescence analysis. Immunohistochemical analysis and 3,3′-diaminobenzidine staining were done according to the manufacturer's instructions (Vector Laboratories), and all primary and secondary antibodies used are listed in Supplementary Table S1. For evaluation of KLK6 protein staining, intensity was graded semiquantitatively (1 = weak, 2 = moderate, 3 = strong). Immunofluorescence staining of paraffin-embedded and cryosections was described elsewhere (6, 17, 18). Stable MCA3D clones were seeded on glass slides and cultured for 24 h. Cells were fixed for 15 min with 4% paraformaldehyde in PBS buffer (pH 7.2). After intensive washing with PBS buffer (pH 7.2), fixed cells were incubated for 30 min with blocking buffer [1% bovine serum albumin (BSA) and 0.5% Triton X-100 in PBS buffer (pH 7.2)]. Afterwards, cells were incubated for 2 h with primary antibodies diluted in incubation buffer [1% BSA and 0.2% Tween 20 in PBS buffer (pH 7.2)]. On intensive washing with washing buffer [0.2% Tween 20 in PBS buffer (pH 7.2)], cells were incubated for 1 h with secondary fluorescence-labeled antibodies diluted in incubation buffer supplemented with 1 μg/mL H33342 (Calbiochem). For staining of the actin cytoskeleton, fixed cells were incubated for 1 h with phalloidin-Alexa Fluor 488 (Invitrogen) diluted in incubation buffer. On intensive washing with washing buffer, stained cells were mounted with Mowiol on glass slides. Image acquisition was done by bright-field or fluorescence microscopy (Leica DMLB microscope) using a digital camera (Nikon digital camera DXM1200) and the Nikon Act-1 software. Image processing was done with the Adobe Photoshop 7.0 software.

Cell proliferation assays. To measure the growth rate of stable MCA3D clones, 1×10^4 cells were plated in 96-well plates and cell numbers were counted at the indicated time points using a cell counter (Beckman Coulter). The cell cycle profile of logarithmic growing cells was analyzed using the BrdU Flow kit (BD Biosciences) according to the manufacturer's instructions, and labeled cells were measured by fluorescence-activated cell sorting analysis (FACSCalibur, BD Biosciences). All experiments were done at least thrice.

Scratch assay. Stable MCA3D clones were seeded in six-well plates and cultured until confluence. On treatment with 20 ng/mL mitomycin C and intensive washing with PBS buffer, the cell monolayer was scratched with a yellow micropipette tip. Images of the same area were taken after scratching and at the indicated time points using phase-contrast microscopy and a digital camera. Relative migration of mock- and Klk6-transfected keratinocytes was calculated from three independent experiments.

Chorioallantoic membrane assay. Fertilized terracotta brown chicken eggs were purchased by a local farmer, and preparation of the chorioallantoic membrane (CAM) was done as described elsewhere (19). Mock control or Klk6-transfected MCA3D cells (1×10^6) were labeled for 5 min with 0.5 nmol/mL carboxyfluorescein diacetate succinimidyl ester (Invitrogen) and applied on the CAM of 11-day-old chicken embryos. After 2 to 3 days of further incubation, the CAM-containing cells were dissected, mounted with a coverslip, and analyzed using laser scanning confocal microscopy (LSM 510 UV microscope, Zeiss) and LSM5 Image Browser software (Zeiss). Image processing was done with Adobe Photoshop 7.0 software.

Spheroid assay. Twenty-four hours after transient transfection with pcDNA3.1-KLK6-Myc/His or parental pcDNA3.1-Myc/His plasmid, 0.2×10^5 to 1×10^5 HEK293 cells were suspended in 20 μL DMEM supplemented with 10% FCS, which was then used for the spheroid assay (hanging drop assay). The drops were plated on the lid of a 6-cm tissue culture dish containing 2 mL DMEM to avoid evaporation and incubated at 37°C and 6% CO_2. On 12-h incubation, spheroids were carefully washed with PBS buffer, labeled with 1 μg/mL H33342, and mounted with Mowiol. Spheroids were counted by fluorescence microscopy (Leica DMLB microscope), and images were taken using a digital camera (Nikon digital camera DXM1200) and the Nikon Act-1 software. Image processing was done with the Adobe Photoshop 7.0 software. For inhibition studies, 20 nM of recombinant

TIMP-1 and TIMP-3 proteins were added to the hanging drops with mock- or KLK6-transfected HEK293 cells.

Statistical procedures. All values unless otherwise indicated are expressed as mean ± SE. Statistical analysis was carried out using a two-tailed Student's unpaired *t* test, and according to conventional criteria, *P* values of <0.05 were considered statistically significant.

Generation of transgenic mice and wound-healing experiments. The cDNA encoding the mouse Klk6-Myc/His fusion protein derived from the pcDNA3.1-Klk6-Myc/His plasmid was cloned in a plasmid with a human *ubiquitin C* promoter (20) and a *lacZ* reporter gene flanked by loxP sequences (ubi-lacZ^{fl}-Klk6). On deletion of the *lacZ* reporter gene by Cre recombinase, efficient Klk6 expression was observed in transiently transfected cells (data not shown). The Transgene Facility of the Deutsches Krebsforschungszentrum Heidelberg used the linearized ubi-lacZ^{fl}-Klk6 plasmid to generate transgenic founders. These mice were crossed with CMV-Cre transgenic animals for at least two generations to allow germ-line recombination and to establish ubi-Klk6 mice that express constitutively ectopic Klk6. Animals were housed in specific pathogen-free and light-controlled, temperature-controlled (21°C), and humidity-controlled (50–60% relative humidity) conditions. Food and water were available *ad libitum*. ubi-Klk6 and ubi-lacZ^{fl}-Klk6 (as controls) littermates were used for full-thickness excision wounding as described previously (17, 18). Transgene generation and wounding experiments were in accordance with the principles and guidelines of the ATBW (officials for animal welfare) and were approved by the Regierungspräsidium Karlsruhe (AZ 103/03 and AZ 127/03).

Results

KLK6 expression levels in human malignancies. To determine KLK6 protein expression in premalignant skin tumors and cutaneous SCC samples of human patients, we did immunohistochemistry on tissue microarrays. Weak immunoreactivity was detected in the epidermis of normal skin with a signal restricted to keratinocytes of the suprabasal epidermis and hair follicles (Fig. 1*A*; data not shown). We found moderate staining for KLK6 in ~49% and strong staining in 10% of premalignant tumors, respectively (Fig. 1*B*). In most of these samples, tumor cells surrounding the cornified inclusions were KLK6 positive. Additionally, immunohistochemical analysis revealed elevated KLK6 protein levels for SCC samples with 46% showing moderate and 28% strong signal intensity (Fig. 1*B*), suggesting a positive correlation between KLK6 expression and malignant progression.

Next, we used hybridization of a cancer profiling array consisting of paired cDNA samples generated from total RNA of multiple tissue samples with a radioactive-labeled *KLK6*-specific probe. Each pair shared a tumor sample and a corresponding normal tissue sample obtained from the same patient. The hybridization confirmed increased *KLK6* transcript levels in two cutaneous SCC samples present on the array (Fig. 1*C, asterisks*). In addition, elevated *KLK6* transcript levels were detected in tumors of the gastrointestinal tract, ovary, and vulva and in malignant melanomas (Fig. 1*C*). Thus, we hypothesized that aberrant expression of this secreted serine proteinase is a common feature of carcinogenesis and might critically contribute to the development and progression of human malignancies.

Altered morphology and proliferation of keratinocytes with ectopic Klk6 expression. To unravel the consequence of enhanced Klk6 expression on epithelial cells, we transfected the mouse keratinocyte cell line MCA3D with an expression plasmid encoding a mouse Klk6-Myc/His-tagged fusion protein. On selection for stable integration, two independent clones (MCA3D-Klk6#1 and MCA3D-Klk6#2) that expressed large amounts of *Klk6* mRNA and exhibited high Klk6 protein levels in the cell culture supernatant compared with mock-transfected controls were chosen for further experiments (Supplementary Fig. S1*A*). Accordingly, we found significant amounts of the active proteinase in the cell culture supernatant as shown by gelatin zymography (data not shown). In contrast to mock-transfected controls, which showed normal epithelial morphology with definitive cell-cell contacts, both MCA3D-Klk6 clones were characterized by a spindle-like cell morphology in concert with a rearrangement of the actin cytoskeleton (Fig. 2*A*). When we seeded control and MCA3D-Klk6 clones at low density and measured total cell numbers for a time period of 10 days, a significantly elevated growth rate was observed for both Klk6-expressing clones from day 5 compared with mock controls (Fig. 2*B*). The difference in the growth rate is most likely

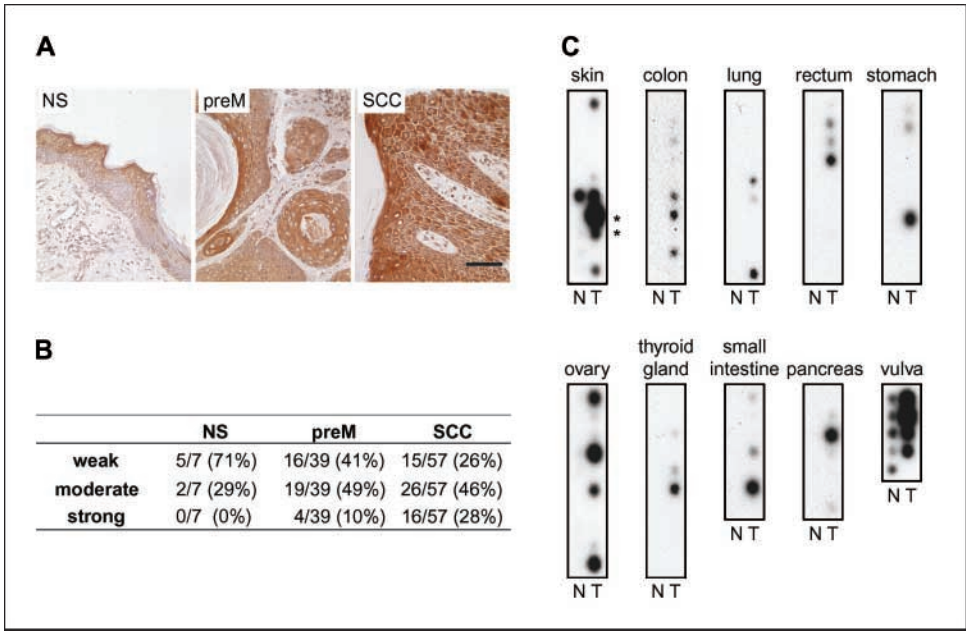

	NS	preM	SCC
weak	5/7 (71%)	16/39 (41%)	15/57 (26%)
moderate	2/7 (29%)	19/39 (49%)	26/57 (46%)
strong	0/7 (0%)	4/39 (10%)	16/57 (28%)

Figure 1. Klk6 expression in human malignancies. *A,* tissue microarrays with specimens of normal skin (*NS*), premalignant skin tumors (*preM*), and SCC were analyzed by indirect immunohistochemistry using a polyclonal anti-KLK6 antibody. The sections were counterstained with hematoxylin. KLK6 protein expression (*brown signal*) is shown for representative images. *Bar*, 100 μm. *B,* quantification of signal intensity for KLK6 protein levels in normal skin, premalignant skin tumors, and SCC determined by indirect immunohistochemistry on tissue microarrays. The table shows the number of samples with weak, moderate, and strong staining for KLK6 protein and, in *parentheses*, the percentage compared with all samples of the indicated stage (normal skin, *n* = 7; premalignant skin tumors, *n* = 39; SCC, *n* = 57). *C,* a cancer profiling array with cDNA of normal (*N*) and tumor samples (*T*) derived from indicated tissues was hybridized with a radioactive-labeled *KLK6*-specific cDNA probe and exposed to an X-ray film. *Asterisks,* SCCs in the skin tumor part.

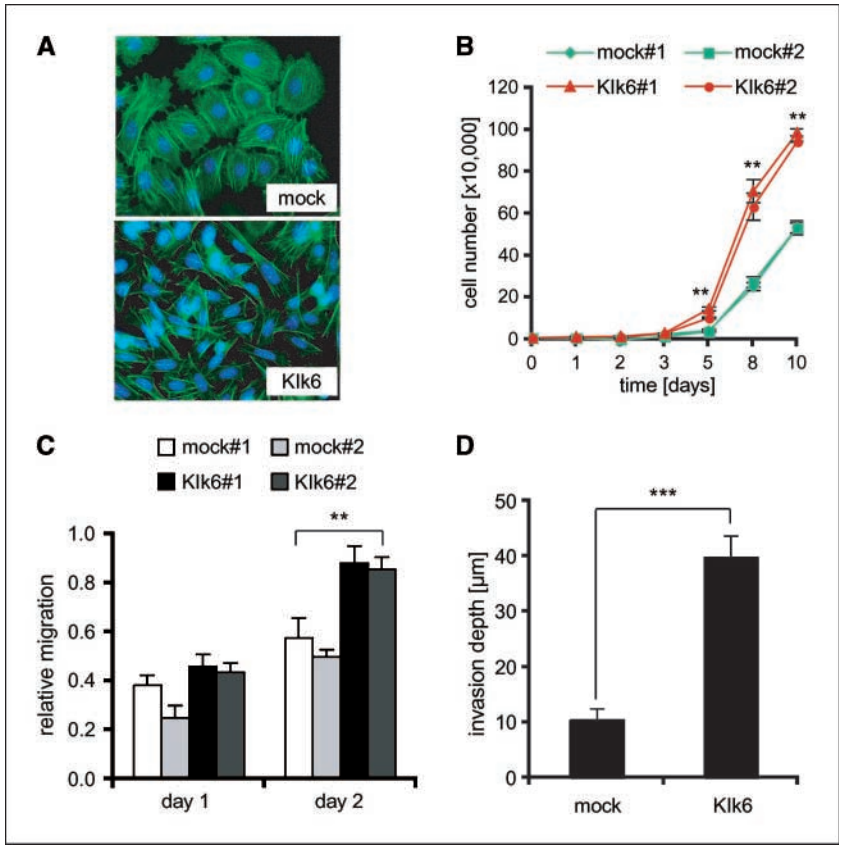

Figure 2. Ectopic Klk6 expression induces spindle-like morphology and accelerates proliferation, migration, and invasion. *A,* mock controls and stable MCA3D-Klk6 keratinocytes were cultured on glass slides and the actin cytoskeleton was stained with phalloidin-Alexa Fluor 488. H33342 was used for nuclear staining and images were done by fluorescence microscopy. *B,* 1×10^4 mock control (*green lines*) and stable MCA3D-Klk6 keratinocytes (*red lines*) were seeded and the cell number was measured at the indicated time points. *Points,* mean value of three independent experiments; *bars,* SE. **, $P < 0.005$. *C,* quantification of relative migration at indicated time points determined by a scratch assay with mock controls (*white* and *light gray columns*) and stable MCA3D-Klk6 keratinocytes (*black* and *dark gray columns*). Cells were grown to a confluent monolayer and treated with mitomycin C to inhibit cell proliferation. The confluent monolayer was wounded by manually scratching with a pipette tip, and following further incubation, the distance between two migrating cell borders was measured over a time period of 2 d (see Supplementary Fig. S2*A*). *Columns,* relative closure of the wounded area as mean value of three independent experiments; *bars,* SE. **, $P < 0.005$. *D,* the same number of fluorescence-labeled mock controls (*mock*) or stable MCA3D-Klk6 keratinocytes (*Klk6*) were seeded on top of the CAM of 11-day-old chicken eggs and cultured further for 2 to 3 d. The cell containing CAM was prepared and laser scanning confocal microscopy was applied to generate consecutive pictures. Cell invasion was quantified by the maximal depth (μm) the cells invade the CAM within the indicated time course (see Supplementary Fig. S2*B*). *Columns,* mean values of two independent experiments that were done with both mock controls and MCA3D-Klk6 clones, respectively; *bars,* SE. ***, $P < 0.0005$.

due to an accelerated cell cycle progression because a bromodeoxyuridine (BrdUrd) incorporation assay revealed more Klk6-expressing cells in S phase (mean value, 50.7%) compared with mock controls (mean value, 25.8%; Supplementary Fig. S1*B*).

Klk6 expression induces keratinocyte migration and invasion. Next, we studied the effect of Klk6 expression on keratinocyte migration and invasion using *in vitro* scratch and *in ovo* CAM assays. To analyze cell migration, confluent monolayers of MCA3D-Klk6 clones and mock controls were treated with mitomycin C to inhibit proliferation and wounded by manually scratching with a pipette tip (Supplementary Fig. S2*A*). Subsequently, the distance between the two migrating cell fronts was measured over a time period of 2 days. We found slightly enhanced migration of MCA3D-Klk6 clones compared with mock

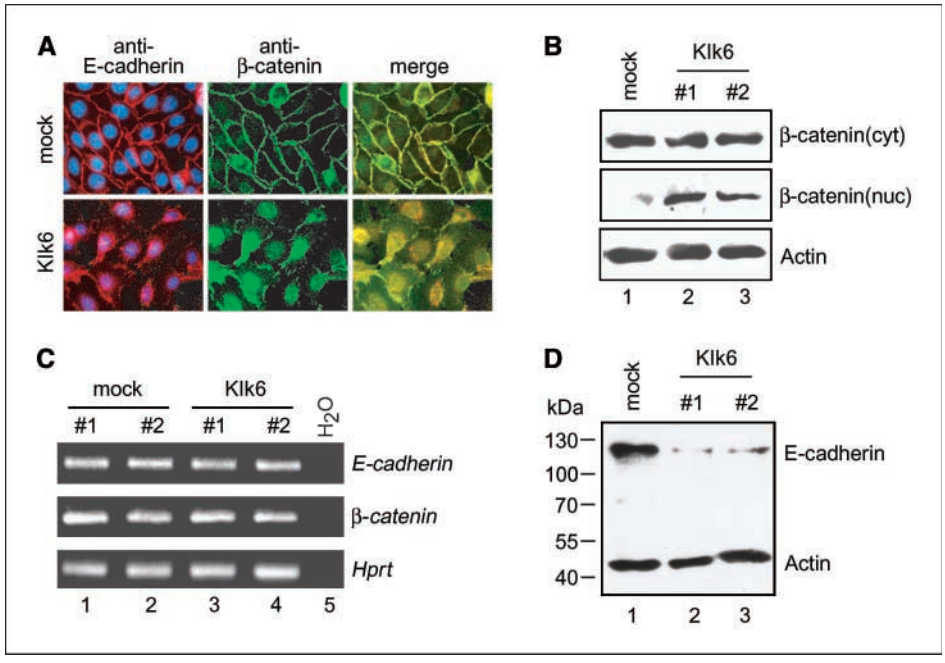

Figure 3. Klk6 expression affects E-cadherin levels and nuclear β-catenin accumulation. *A,* indirect immunofluorescence analysis of mock controls and stable MCA3D-Klk6 keratinocytes using anti-E-cadherin (*left, red signal*) or anti-β-catenin antibodies (*middle, green signal*). Nuclei were counterstained with H33342 and images were done by fluorescence microscopy. *B,* Western blot analysis with cytoplasmic (*cyt*) and nuclear (*nuc*) extracts of a mock control (*lane 1*) and stable MCA3D-Klk6 keratinocytes (*lanes 2* and *3*) using an anti-β-catenin antibody. β-Actin protein levels served as a control for cell extract quantity and quality. *C,* semiquantitative RT-PCR was done with cDNA from mock controls (*lanes 1* and *2*) and stable MCA3D-Klk6 keratinocytes (*lanes 3* and *4*) and specific primers for *E-cadherin* or *β-catenin*. Detection of *Hprt* transcripts served as control for cDNA quantity and quality. *D,* Western blot analysis was done with whole-cell extracts of a mock control (*lane 1*) and stable MCA3D-Klk6 keratinocytes (*lanes 2* and *3*) using an anti-E-cadherin antibody. β-Actin protein levels served as a control for cell extract quantity and quality. *Numbers on the left,* size of marker protein in kDa.

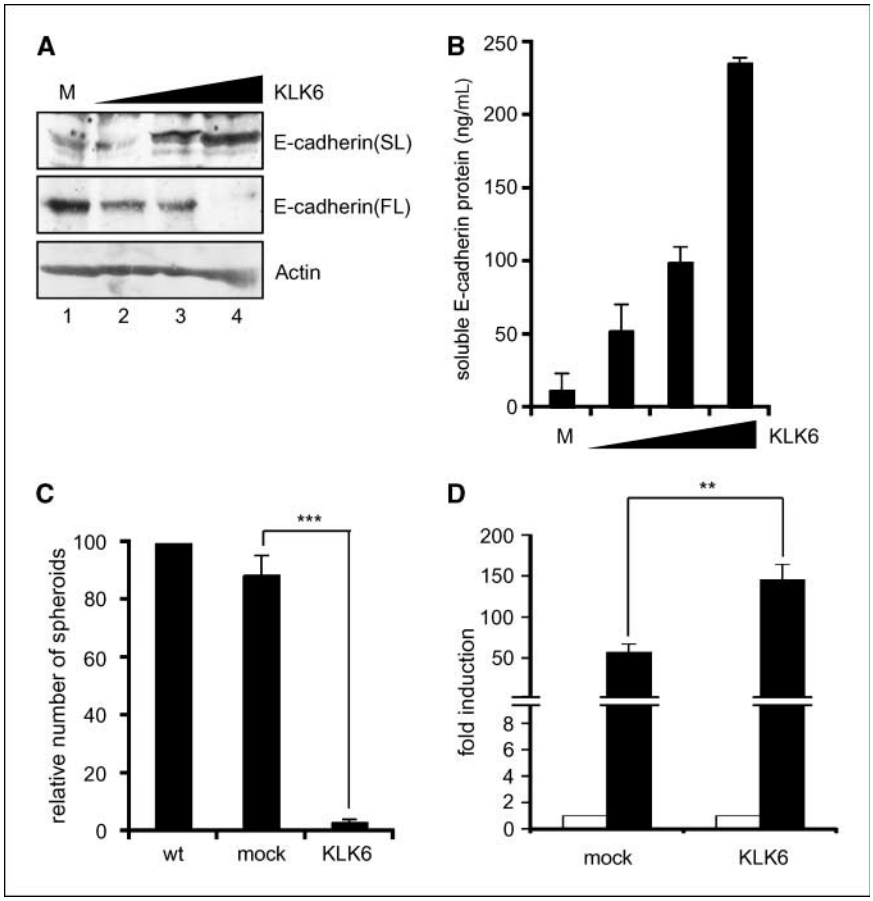

Figure 4. KLK6 induces E-cadherin ectodomain shedding and interferes with cell-cell adhesion. *A,* HEK293 cells were transiently transfected with a control plasmid (*M*) or increasing amounts of a human KLK6 expression plasmid. Whole-cell extracts (*middle* and *bottom*) and cell culture supernatant purified with ConA-Sepharose beads (*top*) were analyzed by Western blot analysis using anti-E-cadherin antibodies that recognized the soluble fragment (*SL*) in the supernatant or the full-length protein (*FL*) in the cell extract, respectively. β-Actin protein levels served as a control for protein extract quantity and quality. *B,* quantification of soluble E-cadherin levels in the supernatant of mock controls and KLK6-transfected HEK293 cells by ELISA. *Columns,* mean values determined in triplicates; *bars,* SE. *C,* spheroid assay was done with nontransfected (*wt*), mock-transfected, and KLK6-transfected HEK293 cells. Cell aggregation was visualized on nuclear staining with H33342 using fluorescence microscopy (see Supplementary Fig. S2*C*), and the amount of spheroids was counted. The total number of spheroids formed by nontransfected cells was set to 100. *Columns,* mean values of four independent experiments; *bars,* SD. ***, $P < 0.0005$. *D,* HEK293 cells were transiently transfected with expression plasmids for KLK6 and TCF reporter plasmids (TCFwt = TOPflash and TCFmut = FOPflash). Luciferase activity was measured 24 h after transfection, and *Renilla* luciferase activity was measured as an internal control for transfection efficiency. Relative light units of TCFmut-transfected cells are set to one. *Columns,* mean of five independent experiments; *bars,* SD. **, $P < 0.005$.

controls after 1 day and a significant increase in migration after 2 days (Fig. 2*C*).

To determine whether ectopic Klk6 expression induces the tissue invasion activity of keratinocytes, the same amount of fluorescence-labeled control cells or MCA3D-Klk6 cells was grafted on top of a chicken CAM, a type I collagen-rich extracellular matrix (ECM) barrier commonly used to study invasive processes. In a time course of 2 to 3 days, both the control and MCA3D-Klk6 cells invade the CAM; however, laser scanning confocal microscopy revealed a 4-fold pronounced invasion potential for MCA3D-Klk6 cells compared with mock controls (Fig. 2*D*; Supplementary Fig. S2*B*).

Klk6 expression affects E-cadherin levels and β-catenin localization. Phenotypic changes in keratinocytes that were observed on ectopic Klk6 expression pointed to a possible impairment in cell-cell adhesion. Hence, we investigated the distribution of cell adhesion molecules in confluent growing cell cultures by immunofluorescence analysis. Using an antibody raised against a cytoplasmic epitope of E-cadherin, we found strong staining for E-cadherin at the membrane of mock controls and a colocalization with β-catenin that represents an integral component of E-cadherin complexes at intercellular adherent junctions (Fig. 3*A*). In contrast, MCA3D-Klk6 clones showed decreased E-cadherin levels at the membrane in concert with cytoplasmic and nuclear accumulation of β-catenin (Fig. 3*A*). Nuclear accumulation of β-catenin was further confirmed by Western blot analysis showing elevated levels in nuclear extracts of MCA3D-Klk6 clones versus mock controls (Fig. 3*B*). Differences in E-cadherin protein levels were not due to altered transcription because semiquantitative RT-PCR revealed comparable amounts of *E-cadherin* transcripts in mock controls and MCA3D-Klk6 clones (Fig. 3*C*). The same was also true for *β-catenin* transcript levels. However, in a Western blot conducted with whole-cell extracts and an anti-E-cadherin antibody raised against an extracellular epitope, we found severely decreased amounts of full-length E-cadherin protein in MCA3D-Klk6 clones compared with mock controls (Fig. 3*D*).

KLK6 expression induces E-cadherin ectodomain shedding and reduces cell-cell adhesion. Recent data showed that human KLK6 was able to activate the proteinase-activated receptor-2 (PAR-2) via proteolytic cleavage, leading to PAR-2–mediated calcium signaling in human HEK293 cells (21–23). It is well established that increased calcium signaling (e.g., by the ionophore ionomycin) influences cell-cell adhesion by E-cadherin; therefore, we assayed E-cadherin levels in cell lysates and supernatants of human HEK293 cells transfected with increasing amounts of a KLK6 expression plasmid. Full-length E-cadherin protein was easily detectable by Western blot analysis in whole-cell extracts of mock-transfected HEK293 cells, whereas a significant reduction was observed in KLK6-expressing cells (Fig. 4*A, middle*). In contrast, elevated levels of soluble E-cadherin were found in supernatants of KLK6-transfected HEK293 cells as measured by Western immunoblot on ConA-Sepharose purification or ELISA with a soluble E-cadherin–specific antibody [Fig. 4*A* (*top*) and *B*]. These data suggest that KLK6 induces E-cadherin ectodomain shedding, resulting in an increase of soluble E-cadherin. Because soluble

E-cadherin interferes with cell-cell adhesion in a paracrine manner, we analyzed the effect of KLK6 expression on cell-cell adhesion doing a spheroid assay with transfected HEK293 cells. In contrast to nontransfected or mock-transfected controls that efficiently aggregate to large spheroids, cells with ectopic KLK6 expression showed impaired cell-cell adhesion and an almost complete loss of spheroid formation (Fig. 4*C*). To analyze whether KLK6-induced E-cadherin ectodomain shedding in HEK293 cells also correlates with nuclear β-catenin translocation, we determined the activation of β-catenin/TCF-dependent transcription in the presence or absence of ectopic KLK6 expression. Cotransfection of HEK293 cells with a KLK6 expression and a TCF-dependent luciferase reporter plasmid (TCFwt-luci) revealed a 3-fold increase in reporter gene activity compared with mock-transfected controls (Fig. 4*D*). In contrast, no difference was measured for a luciferase reporter plasmid (TCFmut-luci) with inactive TCF-binding sites.

KLK6-induced E-cadherin ectodomain shedding requires proteolytic activity of MMPs. In summary, these data show that KLK6 directly or indirectly induces E-cadherin ectodomain shedding and thereby affects cell-cell adhesion and gene expression via β-catenin/TCF. However, the proteolytic activity that has thus far been linked to E-cadherin ectodomain shedding requires different proteinases of the MMP superfamily, particularly a disintegrin and metalloproteinase (ADAM) proteins. Therefore, we assessed whether recombinant TIMPs were capable to interfere with induced E-cadherin ectodomain shedding of HEK293 cells transfected with a KLK6 expression plasmid. Indeed, TIMP-1 and TIMP-3 efficiently reduced the amount of soluble E-cadherin in the supernatant of KLK6-expressing cells (Fig. 5*A*, compare *lane 4* with *lanes 6* and *8* in *top*), whereas full-length E-cadherin detected in total cell lysates was restored to levels of mock controls (Fig. 5*A*, compare *lane 3* with *lanes 6* and *8* in *middle*). Reduced soluble E-cadherin levels in supernatants of TIMP-1– and TIMP-3–treated HEK293 cells transfected with a KLK6 expression plasmid were confirmed by ELISA quantification (data not shown). Finally, we did a spheroid assay with transfected HEK293 cells and recombinant TIMP proteins. In the presence of TIMP-1 or TIMP-3, minor but significant differences in spheroid numbers between KLK6-transfected cells and mock controls were observed (Fig. 5*B*). However, addition of TIMP-1 or TIMP-3 proteins to KLK6-transfected cells increased the amount of spheroids 19- and 16-fold, respectively, whereas no positive effect was observed on mock controls (Fig. 5*B*). These data show that both inhibitors exhibit protective functions, and we concluded that members of the MMP protein family are essential for the cell-cell adhesion defect induced by KLK6.

Several different subtypes of metalloproteinases, including members of the MMP (e.g., MMP7 and MMP9) and of the ADAM family (e.g., ADAM10 and ADAM17), have been implicated in basal and inducible E-cadherin ectodomain shedding. To address the question whether MMP7 and/or MMP9 are critically involved in KLK6-mediated E-cadherin shedding and impaired cell-cell adhesion, we did gelatin zymography with conditioned medium from KLK6-transfected HEK293 cells and mock controls. We found no obvious difference in total or mature amounts of the two gelatinases MMP2 and MMP9 (Supplementary Fig. S3). Moreover, we could not find evidence for activity of latent (28 kDa) or mature MMP7 (19 kDa; data not shown) as was described in MCF-7 cells (24).

Next, we analyzed the activation of ADAM proteinases by Western immunoblotting using specific antibodies that recognize both latent as well as proteolytically processed mature variants on whole-cell extracts of KLK6-transfected HEK293 cells and mock controls. We found increased levels of a 62-kDa variant that corresponds to the mature ADAM10 proteinase in the presence of ectopic KLK6 expression (Fig. 5*C*), whereas no difference was detected for ADAM17 (data not shown), suggesting that ADAM10 is implicated in E-cadherin ectodomain shedding induced by KLK6 expression.

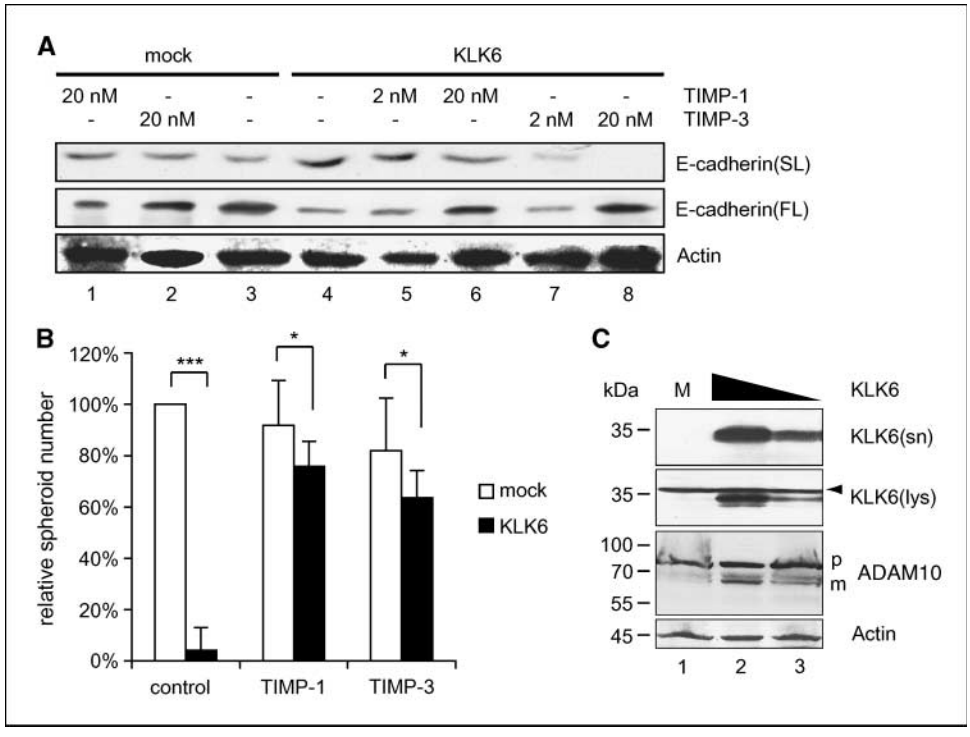

Figure 5. Recombinant TIMP proteins inhibit E-cadherin ectodomain shedding and restore cell-cell adhesion. *A,* mock control (*lanes 1–3*) and KLK6-transfected HEK293 cells (*lanes 4–8*) were incubated without (−) and with 2 or 20 nM recombinant TIMP-1 and TIMP-3 protein, respectively. Whole-cell extracts and supernatants were analyzed by Western blot analysis as described for Fig. 4*A*. *B,* spheroid assay was done and quantified as described for Fig. 4*B* in the absence (control) or presence of recombinant TIMP-1 or TIMP-3 protein. ***, $P < 0.0005$; *, $P < 0.05$. *C,* Western immunoblot analysis with whole-cell extracts and purified proteins from the supernatant of KLK6-transfected HEK293 cells (*lanes 2* and *3*) and mock controls (*M, lane 1*). Expression and secretion of the KLK6-Myc/His fusion protein was confirmed with purified proteins from the cell culture supernatant (*sn*) and total cell lysates (*lys*) using a monoclonal anti-Myc antibody. *Arrowhead,* unspecific background band. Protein levels of the premature (*p*) and the mature (*m*) ADAM10 proteinase were detected with a monoclonal anti-ADAM10 antibody. β-Actin protein levels served as a control for protein extract quantity and quality. *Numbers on the left,* protein size in kDa.

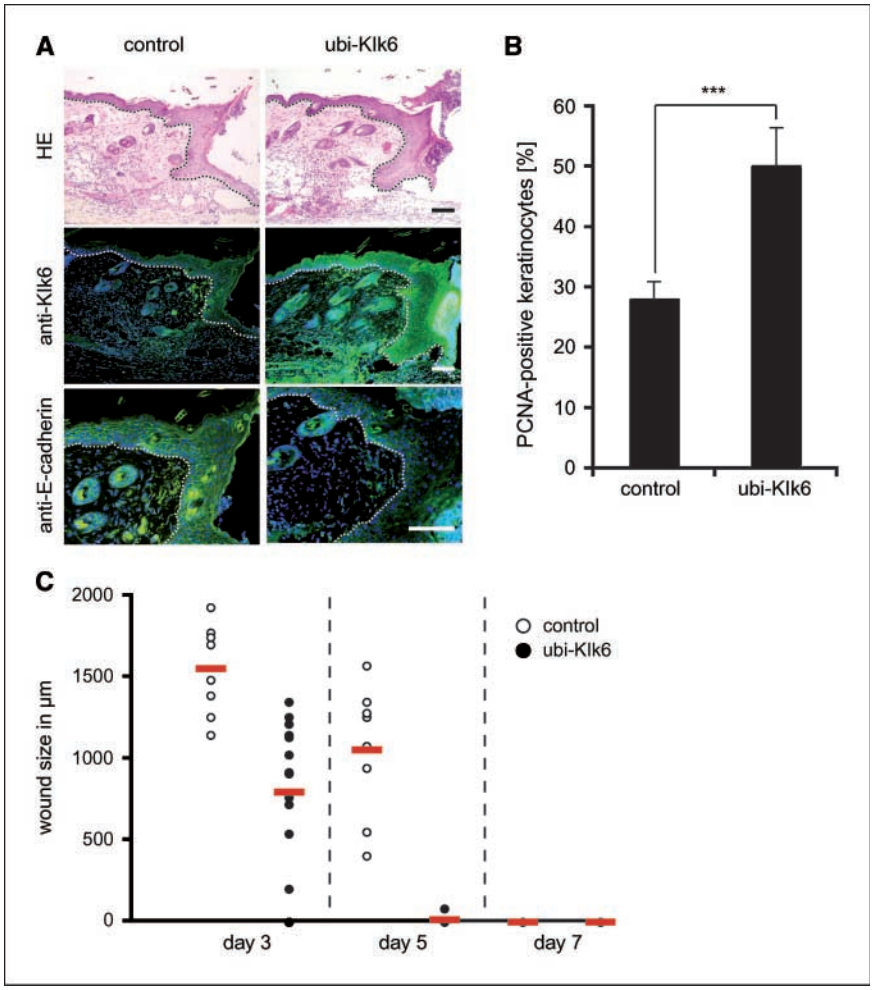

Figure 6. Klk6 induces keratinocyte proliferation and migration in an *in vivo* mouse model. *A,* histology of the adjacent hyperplastic skin of 3-day-old full-thickness excision wounds of control (ubi-lacZ^{fl}-Klk6) and Klk6 transgenic (ubi-Klk6) mice on H&E staining (*HE, top*). Indirect immunofluorescence staining shows Klk6 transgene expression in 3-day-old wounds of ubi-Klk6 animals compared with control littermates (*green signal, middle*) accompanied by decreased E-cadherin protein levels at the membrane of keratinocytes (*green signal, bottom*). *Dashed lines,* border between the epidermis and the dermis. *Bar*, 100 μm. *B,* immunofluorescence staining with a PCNA-specific antibody revealed a higher proliferation rate in epidermal keratinocytes at the hyperplastic wound edge of ubi-Klk6 mice (n = 16) compared with control littermates (n = 9) in 3-day-old wounds. *Columns,* mean values of counted areas; *bars,* SD. ***, $P < 0.0005$. *C,* kinetic of reepithelialization in control and ubi-Klk6 mice determined by the distance of the wound edges at days 3, 5, and 7. *Red bars,* mean values for each genotype at the indicated time point.

Klk6 transgene expression induces keratinocyte proliferation and migration during cutaneous wound healing. Increased keratinocyte proliferation and migration is a hallmark of cutaneous wound healing that represents an appropriate experimental approach to study the *in vivo* consequence of ectopic Klk6 expression. Thus, we generated transgenic mice that express a Klk6-Myc/His fusion protein under the control of the human *ubiquitin C* promoter (ubi-Klk6). These mice were viable and showed no obvious phenotype during embryonic development or homeostasis of epithelial tissues (data not shown). Next, we did full-thickness excision wounds on the back skin and found a strong up-regulation of Klk6 protein levels in skin sections of ubi-Klk6 mice compared with control littermates (Fig. 6*A*). According to the *in vitro* data, enhanced Klk6 expression was associated with reduced E-cadherin levels at the membrane of epidermal keratinocytes. We determined the number of cycling keratinocytes within the hyperplastic area of the wound at different time points by immunofluorescence analysis. Three days after wounding, we found in tissue sections of ubi-Klk6 mice a highly significant increase in the percentage of proliferating cell nuclear antigen (PCNA)-positive keratinocytes compared with wounds of control littermates (Fig. 6*B*). Similar data were also found by immunofluorescence staining for Ki67 (data not shown), supporting the concept that Klk6 accelerates keratinocyte proliferation also *in vivo*. Following the kinetics of wound closure, we observed in wounds of control animals that reepithelialization occurred within 7 days of wounding (Fig. 6*C*), which agrees with published data (18). In contrast, wounds of almost all ubi-Klk6 animals showed a continuous epithelial layer 5 days after wounding, and 3 days after wounding, we found a significant accelerated reepithelialization of wounds from ubi-Klk6 mice compared with wounds of control littermates. These data support our *in vitro* findings that ectopic Klk6 expression promotes keratinocyte proliferation and migration.

Discussion

Kallikreins are implicated in a vast range of normal and pathologic processes, where they either act independently or as part of one or more proteolytic cascades (12). Recently, it has been shown that several kallikreins, including KLK6, are useful biomarkers for common types of human malignancies, and new evidence raises the possibility that some are directly involved with cancer progression (12, 25, 26). In the past, we identified the mouse orthologue of human *KLK6* as a TPA-inducible gene in keratinocytes of mouse back skin and found enhanced expression during multistage skin carcinogenesis in an *in vivo* tumor model (5). Our current study extended this analysis, showing increased KLK6 protein levels in tissue sections of human skin cancer and a correlation with tumor progression. Moreover, we found enhanced transcription in tumors of the gastrointestinal tract, ovary, and vulva and in malignant melanomas. In line with these findings, KLK6 was found to be frequently overexpressed in human

epithelial cancers and to be associated with cancer progression (12, 27, 28). Furthermore, KLK6 was described as one of the most promising ovarian cancer biomarker among the kallikrein family and is discussed as having some value in colon cancer diagnostics (29–33).

Apparently, studies on the molecular function of KLK6 and its *in vivo* substrates during neoplastic transformation of epithelial cells will highlight its role in cancer promotion and progression. We found that ectopic KLK6 expression by epithelial cells affects proliferation, adhesion, migration, and invasion, which are all important cellular processes critically implicated in cancer development. Similar findings were reported recently for a gastric cancer cell line, which inherently expressed high KLK6 levels. Nagahara et al. (27) showed in this study that KLK6 suppression by a RNA interference strategy markedly reduced cell growth, proliferation, and invasiveness.

Although *in vitro* proteinase assays showed that KLK6 degrades major components of the basal membrane and ECM, such as fibrinogen, collagen type I and IV, fibronectin, vitronectin, and laminin (34–36), the *in vivo* targets of KLK6 during carcinogenesis remained elusive. Here, we could show that KLK6 expression affects E-cadherin protein levels at the cell membrane accompanied by cytoplasmic and nuclear accumulation of β-catenin. Reduced E-cadherin levels were not due to decreased transcription but caused by an increased ectodomain shedding induced by KLK6. Ectodomain shedding is a process by which the extracellular domain of a transmembrane molecule is proteolytically removed from the cell surface. In the case of E-cadherin, ectodomain shedding results in a soluble E-cadherin fragment, which inhibits normal E-cadherin function in a paracrine manner promoting migration and invasion of tumor cells (37–39). Thus far, several MMPs (e.g., MMP7 and MMP9) and specifically ADAMs (e.g., ADAM10 and ADAM17) have been implicated in ectodomain shedding of E-cadherin (37, 40–42). MMPs and ADAMs are synthesized as latent enzymes that are secreted or membrane associated and must be proteolytically processed to their active form. Because proenzymes can be activated at least in part by trypsin-like serine proteinases, one could ask the question of whether induced E-cadherin ectodomain shedding is the consequence of KLK6 function on MMP and/or ADAM proteinase activity. Indeed, recombinant TIMP-1 and TIMP-3 block KLK6-induced E-cadherin ectodomain shedding and rescues the cell-cell adhesion defect in an *in vitro* spheroid assay. Whereas MMP expression or function (e.g., MMP2, MMP7, or MMP9) was not altered in the presence of ectopic KLK6, we found that KLK6 expression is associated with ADAM10 activation from its latent to its mature variant. Accordingly, ADAM10 has been shown to mediate both basal and inducible E-cadherin ectodomain shedding and to regulate epithelial cell-cell adhesion, migration, as well as subcellular β-catenin localization and downstream signaling (37). Moreover, the postulated proteolytic cleavage site in the latent ADAM10 protein shares some similarities with peptide sequences that have been found to be efficient KLK6 substrates (21).

Recent data show that KLK6 was also able to activate PAR-2 due to proteolytic cleavage, leading to PAR-2–mediated calcium signaling in human HEK293 cells (21–23). It is well established that increased calcium signaling (e.g., by the ionophore ionomycin) results in rapid E-cadherin ectodomain shedding and influences cell-cell adhesion by E-cadherin. Thus, it will be a major challenge for the future to investigate whether the newly identified KLK6-PAR axis triggers calcium signaling in epithelial tumor cells, resulting in an induction of E-cadherin ectodomain shedding via an ADAM10-dependent manner and thereby critically contributing to tumor cell malignancy.

As most data about KLK6 function and substrate identification have been based on *in vitro* biochemical and cell culture model systems, more direct evidence is needed to determine the *in vivo* role of KLK6. Keratinocyte proliferation and migration is a hallmark of cutaneous wound healing. An increase of endogenous *Klk6* transcripts was recently found in samples derived from full-thickness excision wounds of mouse back skin.[3] Elevated Klk6 protein levels were detected in both mitotic keratinocytes at the border of the wound as well as some keratinocytes at the migration front. Detailed analysis of transgenic mice with Klk6 transgene expression in skin confirmed enhanced keratinocyte proliferation and migration accompanied by an accelerated reepithelialization. Again, this phenotype is associated with reduced E-cadherin levels on the membrane of epidermal keratinocytes at the hyperplastic wound edge.

In summary, our data strengthen the idea that KLK6 represents not only a novel biomarker for tumor diagnosis and management but also a promising therapeutic target. The functional and clinical implications of KLK6 in the onset and progression of malignant disease will certainly be a key focus of future cancer research.

[3] R. Mueller and J. Hess, unpublished data.

Acknowledgments

Received 2/14/2007; revised 5/29/2007; accepted 6/8/2007.

Grant support: Research Training Network Program of the European Community grant HPRN-CT2002-00256 (P. Angel); German Ministry for Education and Research, National Genome Research Network NGFN-2, 01GS0460/01GR0418 (P. Angel); and Deutsche Forschungsgemeinschaft grant SFB589, Teilprojekt P11 (K. Breuhahn).

The costs of publication of this article were defrayed in part by the payment of page charges. This article must therefore be hereby marked *advertisement* in accordance with 18 U.S.C. Section 1734 solely to indicate this fact.

We thank Marina Schorpp-Kistner, Michael Rogers, and Christoffer Gebhardt for critical discussion and reading of the manuscript; Andre Nollert, Angelika Krischke, and Elisabeth Specht-Delius for excellent technical assistance; Ulrich Kloz and Franciscus van der Hoeven for generation of the transgenic mice; the National Center for Tumor Diseases Heidelberg for material support; Michael Blaber (Institute of Molecular Biophysics, Tallahassee, FL) for the polyclonal anti-MSP antibody; Christoffer Gebhardt for the help with the tissue microarray analysis; Haymo Kurz (Institute of Anatomy II, University of Freiburg, Freiburg, Germany) for the help with the CAM assay; and Herbert Spring (Deutsches Krebsforschungszentrum) for information technology assistance.

References

1. Owens DM, Watt FM. Contribution of stem cells and differentiated cells to epidermal tumours. Nat Rev Cancer 2003;3:444–51.
2. Hanahan D, Weinberg RA. The hallmarks of cancer. Cell 2000;100:57–70.
3. Marks F, Furstenberger G. The conversion stage of skin carcinogenesis. Carcinogenesis 1990;11:2085–92.
4. Yuspa SH. The pathogenesis of squamous cell cancer: lessons learned from studies of skin carcinogenesis. J Dermatol Sci 1998;17:1–7.
5. Breitenbach U, Tuckermann JP, Gebhardt C, et al. Keratinocyte-specific onset of serine protease BSSP expression in experimental carcinogenesis. J Invest Dermatol 2001;117:634–40.
6. Gebhardt C, Breitenbach U, Richter KH, et al. c-Fos-dependent induction of the small Ras-related GTPase Rab11a in skin carcinogenesis. Am J Pathol 2005;167:243–53.
7. Gebhardt C, Breitenbach U, Tuckermann JP, Dittrich BT, Richter KH, Angel P. Calgranulins S100A8 and

S100A9 are negatively regulated by glucocorticoids in a c-Fos-dependent manner and overexpressed throughout skin carcinogenesis. Oncogene 2002;21:4266–76.
8. Hummerich L, Muller R, Hess J, et al. Identification of novel tumour-associated genes differentially expressed in the process of squamous cell cancer development. Oncogene 2006;25:111–21.
9. Rhiemeier V, Breitenbach U, Richter KH, et al. A novel aspartic proteinase-like gene expressed in stratified epithelia and squamous cell carcinoma of the skin. Am J Pathol 2006;168:1354–64.
10. Schlingemann J, Hess J, Wrobel G, et al. Profile of gene expression induced by the tumour promotor TPA in murine epithelial cells. Int J Cancer 2003;104:699–708.
11. Lundwall A, Band V, Blaber M, et al. A comprehensive nomenclature for serine proteases with homology to tissue kallikreins. Biol Chem 2006;387:637–41.
12. Borgono CA, Diamandis EP. The emerging roles of human tissue kallikreins in cancer. Nat Rev Cancer 2004; 4:876–90.
13. Paliouras M, Diamandis EP. The kallikrein world: an update on the human tissue kallikreins. Biol Chem 2006; 387:643–52.
14. Hess J, Porte D, Munz C, Angel P. AP-1 and Cbfa/runt physically interact and regulate parathyroid hormone-dependent MMP13 expression in osteoblasts through a new osteoblast-specific element 2/AP-1 composite element. J Biol Chem 2001;276:20029–38.
15. Andrecht S, Kolbus A, Hartenstein B, Angel P, Schorpp-Kistner M. Cell cycle promoting activity of JunB through cyclin A activation. J Biol Chem 2002;277: 35961–8.
16. Billion K, Ibrahim H, Mauch C, Niessen CM. Increased soluble E-cadherin in melanoma patients. Skin Pharmacol Physiol 2006;19:65–70.
17. Florin L, Knebel J, Zigrino P, et al. Delayed wound healing and epidermal hyperproliferation in mice lacking JunB in the skin. J Invest Dermatol 2006;126: 902–11.
18. Hartenstein B, Dittrich BT, Stickens D, et al. Epidermal development and wound healing in matrix metalloproteinase 13-deficient mice. J Invest Dermatol 2006;126:486–96.
19. Augustin HG. Methods in endothelial cell biology. Berlin (Germany): Springer-Verlag; 2004.
20. Schorpp M, Jager R, Schellander K, et al. The human ubiquitin C promoter directs high ubiquitous expression of transgenes in mice. Nucleic Acids Res 1996;24:1787–8.
21. Angelo PF, Lima AR, Alves FM, et al. Substrate specificity of human kallikrein 6: salt and glycosaminoglycan activation effects. J Biol Chem 2006;281:3116–26.
22. Oikonomopoulou K, Hansen KK, Saifeddine M, et al. Proteinase-activated receptors, targets for kallikrein signaling. J Biol Chem 2006;281:32095–112.
23. Oikonomopoulou K, Hansen KK, Saifeddine M, et al. Proteinase-mediated cell signalling: targeting proteinase-activated receptors (PARs) by kallikreins and more. Biol Chem 2006;387:677–85.
24. Wang F, Reierstad S, Fishman DA. Matrilysin overexpression in MCF-7 cells enhances cellular invasiveness and pro-gelatinase activation. Cancer Lett 2006;236: 292–301.
25. Obiezu CV, Diamandis EP. Human tissue kallikrein gene family: applications in cancer. Cancer Lett 2005; 224:1–22.
26. Diamandis EP, Yousef GM. Human tissue kallikreins: a family of new cancer biomarkers. Clin Chem 2002;48: 1198–205.
27. Nagahara H, Mimori K, Utsunomiya T, et al. Clinicopathologic and biological significance of kallikrein 6 overexpression in human gastric cancer. Clin Cancer Res 2005;11:6800–6.
28. Ogawa K, Utsunomiya T, Mimori K, et al. Clinical significance of human kallikrein gene 6 messenger RNA expression in colorectal cancer. Clin Cancer Res 2005;11: 2889–93.
29. Tanimoto H, Underwood LJ, Shigemasa K, Parmley TH, O'Brien TJ. Increased expression of protease M in ovarian tumors. Tumour Biol 2001;22:11–8.
30. Diamandis EP, Scorilas A, Fracchioli S, et al. Human kallikrein 6 (hK6): a new potential serum biomarker for diagnosis and prognosis of ovarian carcinoma. J Clin Oncol 2003;21:1035–43.
31. Diamandis EP, Yousef GM, Soosaipillai AR, Bunting P. Human kallikrein 6 (zyme/protease M/neurosin): a new serum biomarker of ovarian carcinoma. Clin Biochem 2000;33:579–83.
32. Hoffman BR, Katsaros D, Scorilas A, et al. Immunofluorometric quantitation and histochemical localisation of kallikrein 6 protein in ovarian cancer tissue: a new independent unfavourable prognostic biomarker. Br J Cancer 2002;87:763–71.
33. Yousef GM, Borgono CA, Popalis C, et al. *In-silico* analysis of kallikrein gene expression in pancreatic and colon cancers. Anticancer Res 2004;24:43–51.
34. Ghosh MC, Grass L, Soosaipillai A, Sotiropoulou G, Diamandis EP. Human kallikrein 6 degrades extracellular matrix proteins and may enhance the metastatic potential of tumour cells. Tumour Biol 2004;25:193–9.
35. Magklara A, Mellati AA, Wasney GA, et al. Characterization of the enzymatic activity of human kallikrein 6: autoactivation, substrate specificity, and regulation by inhibitors. Biochem Biophys Res Commun 2003;307: 948–55.
36. Bernett MJ, Blaber SI, Scarisbrick IA, Dhanarajan P, Thompson SM, Blaber M. Crystal structure and biochemical characterization of human kallikrein 6 reveals that a trypsin-like kallikrein is expressed in the central nervous system. J Biol Chem 2002;277:24562–70.
37. Maretzky T, Reiss K, Ludwig A, et al. ADAM10 mediates E-cadherin shedding and regulates epithelial cell-cell adhesion, migration, and β-catenin translocation. Proc Natl Acad Sci U S A 2005;102:9182–7.
38. Reiss K, Ludwig A, Saftig P. Breaking up the tie: disintegrin-like metalloproteinases as regulators of cell migration in inflammation and invasion. Pharmacol Ther 2006;111:985–1006.
39. Ii M, Yamamoto H, Adachi Y, Maruyama Y, Shinomura Y. Role of matrix metalloproteinase-7 (matrilysin) in human cancer invasion, apoptosis, growth, and angiogenesis. Exp Biol Med 2006;231:20–7.
40. Davies G, Jiang WG, Mason MD. Matrilysin mediates extracellular cleavage of E-cadherin from prostate cancer cells: a key mechanism in hepatocyte growth factor/scatter factor-induced cell-cell dissociation and *in vitro* invasion. Clin Cancer Res 2001;7:3289–97.
41. Lee KH, Choi EY, Hyun MS, et al. Association of extracellular cleavage of E-cadherin mediated by MMP-7 with HGF-induced *in vitro* invasion in human stomach cancer cells. Eur Surg Res 2007;39:208–15.
42. Symowicz J, Adley BP, Gleason KJ, et al. Engagement of collagen-binding integrins promotes matrix metalloproteinase-9-dependent E-cadherin ectodomain shedding in ovarian carcinoma cells. Cancer Res 2007;67: 2030–9.